Simulation of Oxford University Gun Tunnel performance using a quasi-one-dimensional model

D. R. Buttsworth
Faculty of Engineering and Surveying
University of Southern Queensland
Toowoomba, Australia 4350
buttswod@usq.edu.au

P.A. Jacobs
Department of Mechanical Engineering
University of Queensland
Brisbane 4072, Australia

T. V. Jones
Department of Engineering Science
Oxford University
Oxford OX1 3PJ, England

Abstract

The performance of the Oxford University Gun Tunnel has been estimated using a quasi-one-dimensional simulation of the facility gas dynamics. The modelling of the actual facility area variations so as to adequately simulate both shock reflection and flow discharge processes has been considered in some detail. Test gas stagnation pressure and temperature histories are compared with experimental measurements at two different operating conditions – one with nitrogen and the other with carbon dioxide as the test gas. It is demonstrated that both the simulated pressures and temperatures are typically within 3% of the experimental measurements.

keywords: gun tunnel, impulse facility, CFD, facility simulation

1 Introduction

Computational modelling of impulse facility operation can enhance the understanding of important flow processes and assist in the identification of the flow conditions that are produced by such facilities. Such modelling can also be used as an aid in the identification of new operating conditions or the design of new or modified facilities.

Two- or three-dimensional modelling potentially provides detailed information on important flow processes which cannot be accurately captured using one-dimensional simulations (eg, [Petrie-Repar and Jacobs (1998)], and [Chang and Kim (1995)]). However, one-dimensional simulations are far less expensive and are sufficient in many situations depending on type of effects that need to be modelled.

A number of different quasi-one-dimensional numerical formulations for the solution of impulse facility operation have been described by [Groth et al. (1991)], [Jacobs (1994)], and [Tani et al. (1994)]. In such studies, the simulated results are usually compared with experimental pressure measurements, and "good" agreement is often claimed. While the simulated pressure levels may coincide with measurements over some portion of the run, significant deviations are often observed.

For example, the reflected shock tunnel simulations of [Jacobs (1994)] and [Tani et al. (1994)] typically produce pressure histories that are within 10% of the experimental measurements over the period of useful test flow produced by the facility. However, substantial differences between the simulated and experimental shock compression processes can usually be observed within either the pressure history or shock speed comparisons. Hence, there may well be substantial errors in the simulated flow temperatures even if the simulated and experimental pressure levels are in agreement during the useful test time produced by the facilities.

Similarly, with the simulation of gun tunnel performance describe by [Groth et al. (1991)], differences between the simulated and measured pressures of around 25% can be observed during the early stages of the shock compression process. Towards the end of the flow produced by the gun tunnel, the simulated and measured pressure levels are in much closer agreement. However, inaccurate simulation of the earlier shock compression process may lead to errors in the estimated flow temperature even if pressures are subsequently in agreement because the shock compression is not isentropic.

Possible causes of the differences between simulation and experiment observed in these previous studies include: (1) multi-dimensional effects; (2) inaccurate loss modelling; and (3) inaccurate area variation modelling. Clearly, multi-dimensional effects are difficult to accurately simulate using a quasi-one-dimensional model. Previous efforts to improve loss modelling has yielded good results (eg, [Doolan and Jacobs (1996)]). However, little effort has been devoted to the equally significant issue of modelling cross sectional area variations along the length of a facility. Quasi-one-dimensional schemes require gradual area variations for accurate simulation of flow discharge but actual facility area variations are often rapid and should be treated as such in order to accurately simulate wave transmission and reflection processes.

In the current article, the performance of the Oxford University Gun Tunnel is simulated using the Lagrangian formulation described by [Jacobs (1994)]. Paricular attention is given to the problem of modelling area changes for accurate simulation of both flow discharge and wave trans-

mission/reflection processes. Previous impulse facility studies have primarily gauged success through comparison of simulated and measured pressure histories. However, in the current work, comparisons are made between the simulated and measured pressures *and* temperatures in order to properly assess the simulation of the flow state produced by the Oxford University Gun Tunnel.

2 Facility and Instrumentation

2.1 Facility Dimensions and Operation

The principal dimensions of the Oxford University Gun Tunnel are presented in Table 1. The piston is made from a graphite impregnated nylon with a length of 30mm and a mass of around 80grams. The facility is illustrated schematically in Fig. 1, and the cross sectional area variations in the transition region between the driver and barrel, and within the Mach 7 nozzle contraction are illustrated in Fig. 2. The distance x in Fig. 2 is the distance along the facility measured relative to the closed-off end of the driver.

Prior to a run, the barrel, test section and dump tank are evacuated to around 1kPa. The test section is isolated from the barrel with a light plastic diaphragm (the secondary diaphragm) and the barrel is filled with the required test gas (nitrogen or carbon dioxide in the present work). Two scored aluminium diaphragms (separated by a small volume, the breech) isolate the driver and the barrel sections of the gun tunnel (Fig. 1 and 2a). Each of these primary aluminium diaphragms is designed to fail with a pressure difference of just over half of the required driver pressure. The driver section is filled with compressed air to the required pressure with the breech maintained at about half the driver pressure during the driver filling process. To initiate a run, the breech volume is vented to atmosphere, causing the diaphragms to rupture.

2.2 Instrumentation

The Mach 7 nozzle reservoir pressure history during each gun tunnel run was measured at a location 150mm upstream of the barrel end using a piezo electric pressure transducer (Fig. 1). Based on calibrations of the pressure transducer and associated charge amplifier, the estimated uncertainty in the measured pressures is $\pm 1\%$.

Measurements of the flow stagnation temperature were made at the Mach 7 nozzle exit (Fig. 1) with a transient thin film heat flux probe device that has been described in detail by [Buttsworth and Jones (1998)]. Briefly however, the technique relies on the operation of the stagnation point heat flux probes at a number of different probe temperatures. By doing this, a measurement of flow stagnation temperature is obtained that is independent of the probe heat transfer coefficient. The uncertainty in the flow stagnation temperature identified with this device is estimated as ± 10K in the current application.

2.3 Initial Conditions

The initial filling pressures for the gun tunnel conditions considered in the present article are given in Table 2. The initial temperature of the test gas immediately prior to shock compression was

not measured directly but is estimated as close to the ambient temperature of the gun tunnel steel and laboratory environment – 291K with an uncertainty of ±2K. This appears reasonable given the relatively slow barrel filling process and the length of time (about 10 minutes) between completion of the filling and the gun tunnel run.

The temperature of the air driver immediately prior to gun tunnel operation was not measured but it may be substantially higher than the ambient temperature because the driver filling process was rapid and was completed only just prior to gun tunnel operation. With an assumed driver temperature of 291K, the simulated arrival of the reflected driver expansion fan at the pressure transducer station was approximately 3ms late (relative to that indicated by the pressure measurements) for the nitrogen test gas condition. Similarly, the simulated piston stopping shock (which reflects off the driver-barrel transition region) arrived back at the pressure transducer station about 3ms later than indicated by the pressure measurements for the nitrogen condition. As both wave systems take approximately the same time to travel through the driver gas (around 60ms), it was decided to increase the initial simulated driver temperature by the factor $(63/60)^2$ to 321K.

3 Numerical Model

3.1 Background

The numerical model used in the present work is the Lagrangian formulation that has been described in some detail by [Jacobs (1994)]. Briefly however, the area variation along the length of the facility is specified as are the initial conditions of the gas slugs in each region. Each gas slug is divided into a number of control-mass cells with different downstream and upstream interface areas when required. The Riemann solver described by [Jacobs (1992)] is used to identify the flow states at the cell interfaces during each time step while heat and mass transfer in the wall boundary layers appears as source terms in the momentum and energy equations. Pistons (if present) are modelled as point masses with gas pressures acting on the front and back surfaces. State quantities for the gas cells and pistons are advanced in time using a predictor-corrector scheme.

A number of additional features have been developed since the original publication of [Jacobs (1994)] including a boundary layer mass entrainment model to improve the simulation of the contact surface trajectories in shock and expansion tubes, [Doolan and Jacobs (1996)].

3.2 Losses

The modelling of viscous shear losses and heat transfer from each gas cell to the tube wall closely follows the approach adopted by [Groth et al. (1991)]. The shear losses are determined by computing a friction factor based on steady incompressible pipe flow, and the heat transfer follows from the Reynolds analogy, [Jacobs (1994)].

The calculation of pressure losses due to changes in the tube cross sectional area also follows the approach of [Groth et al. (1991)] in which head loss coefficients are distributed over a finite length of the tube. Head loss coefficients are estimated for each contraction and expansion from steady

incompressible results that can be found in many fluids text-books.

For the simulation of the Oxford University Gun Tunnel, a head loss coefficient of $K_L = 1.4$ in total was distributed between $x = 5.523$ and $x = 5.901$m (Fig. 2a). Strictly, a total value of $K_L = 0.8$ only can be identified based on the various abrupt area changes that occur in the transition region and the steady incompressible (text-book) results. However, the additional loss of $K_L = 0.6$ was included to improve the simulation of the measured pressure levels. This additional loss can be justified because: (1) there are actually two primary diaphragms in the transition region which are not otherwise modelled; and (2) losses due to piston friction have been neglected.

3.3 Area Variations

Along the length of impulse facilities, there are frequently discontinuous cross sectional area variations. The most significant change in section in the Oxford University Gun Tunnel occurs between the end of the barrel and the throat of the Mach 7 nozzle (Fig. 2b). To accurately capture the shock reflection process at the end of the barrel it is desirable to keep the rate of area reduction as large as possible. However, the quasi-one-dimensional simulation requires gradual area transitions in order to accurately calculate the flow discharge.

The current approach has been to model the Mach 7 nozzle contraction using an area variation that causes the length of each control mass cell to increase at a constant fraction of the forward velocity as it accelerates through the contraction. This situation can be described as,

$$\frac{dl}{dt} = C_1 u \tag{1}$$

where l is the cell length, t is the time, C_1 is a constant, and u is the local gas (cell) velocity. Since $dx/dt = u$ and $\rho l A = \rho^* l^* A^*$ (the mass in each cell is constant), (1) can be written in nondimensional form as:

$$C_1 \frac{x}{l^*} = \frac{\rho^*}{\rho}\frac{A^*}{A} - 1 \tag{2}$$

where x is the distance from the nozzle throat, ρ is the density, A is the cross sectional flow area, and $*$ indicates the critical (throat) condition.

An alternative approach for modelling discontinuous area variations is an area distribution based on a constant fractional area change across the cell during its progression through the contraction. This criterion can be written as,

$$\frac{dA}{dx} = C_2 \frac{A}{l} \tag{3}$$

and since $\rho l A = \rho^* l^* A^*$, (3) becomes,

$$C_2 \frac{x}{l^*} = \int_1^{AR} \frac{\rho^*}{\rho} \left(\frac{A^*}{A}\right)^2 d\left(\frac{A}{A^*}\right) \tag{4}$$

where AR is the area ratio at the distance x from the contraction throat.

For a given γ, the ratio of specific heats, the right hand sides of both (2) and (4) are functions of the contraction area ratio only. The area distributions described by (2) and (4) are plotted in Fig. 3 for $\gamma = 1.4$.

If $C_1 = C_2$, the change in cell length criterion (2) produces a more gradual contraction than the change in cross sectional area criterion (2), as illustrated in Fig. 3. The two criterion produce approximately the same contraction profile if $C_2 \approx 0.69C_1$. A simulated contraction designed so that each cell increases in length at a rate of (say) 10% of its forward velocity ($C_1 = 0.1$) will cause an area change across each cell of approximately 6.9% ($C_2 = 0.069$) as it progresses through the contraction.

3.4 Grid and Grid Refinement

To identify appropriate levels of grid refinement for the Lagrangian formulation in the current application, the discretisation of two particular flow regions was considered: (1) the driver-barrel transition region; and (2) the Mach 7 nozzle contraction.

The driver gas was divided into regions of coarse and fine cells. The coarse region consisted of 50 cells distributed between $x = 0$ and 4.600m; the fine region consisted of 600 cells distributed between $x = 4.600$ and 5.861m. The fine region was introduced so that the discharge of driver gas into the barrel could be simulated in an accurate and efficient manner.

The driver-barrel transition region grid refinement study considered the nitrogen test gas case and focussed on the piston velocity as the parameter of interest. Immediately prior to deceleration by the reflected shock, the piston velocity was 422.56, 418.09, and 417.46m/s for 150, 300, and 600 cells (respectively) distributed within the fine region. These results indicate a Richardson Extrapolation error estimate for the 600 cell resolution case of around 0.03%, or 0.1% in terms of the grid convergence index suggested by [Roache (1994)].

For the Mach 7 nozzle contraction grid refinement study, a Ludwieg tube arrangement was simulated so that the nozzle discharge obtained from the numerical solution could be compared with the analytical solution. Results are reported in Fig. 4 in terms of average values of C_1 associated with two different contraction profiles. The first profile was a piecewise linear approximation to the smooth contraction described by (2) and is illustrated in Fig. 2b. The second profile was a cubic contraction in tube diameter over the same distance as the first profile. The cubic profile had a zero slope at the start and finish of the contraction.

The vertical bars at each point in Fig. 4 indicate the peak-to-peak noise levels that are generated by the cells as they expand in the axial direction during the contraction process. The noise produced by the contraction designed using (2) is higher than that produced by the cubic contraction. The noise level for the contraction designed using (2) becomes acceptable (peak-to-peak noise $< 1\%$ of the actual mass flow) for values of $C_1 < 0.3$. Although the cubic profile produced less noise, the mass flow errors are much higher for a given level of cell refinement (Fig. 4). Another consideration weighing heavily against the use of a cubic profile is that the shock reflection processes will not be simulated as accurately because of the unnecessarily gradual start to the contraction.

The mass flow error is less than 1% for the the contraction designed using (2) for $C_1 < 0.13$

(Fig. 4). To produce such a level of refinement during the full gun tunnel simulation, the test gas slugs were divided into 600 cells of equal mass.

4 Results

4.1 Pressure

Simulations of the nitrogen and carbon dioxide test gas conditions are compared with experimental measurements of barrel pressure and nozzle exit stagnation temperature in Fig. 5 and 6. The time scale in these figures is referenced to the release of the piston in the simulation. Acquisition of the experimental data was triggered using the barrel pressure signal so the experimental data in Fig. 5 and 6 were aligned on this time scale by matching the experimental incident shock arrival time to the simulated result.

The period normally identified as the test time is illustrated in Fig. 5a and 6a. During the test time, the simulated pressures are within 3% of the experimental measurements for the nitrogen test gas condition and within 1.5% for the carbon dioxide test condition, neglecting the simulated feature described as "piston passing". This feature indicates the simulated time taken by the piston to pass the station 150mm upstream of the barrel end (the pressure transducer station). The average error of 3% is representative of the overall agreement of simulated and measured pressures throughout the duration of the Mach 7 nozzle flow for both the nitrogen and carbon dioxide conditions.

The magnitude of the pressure changes associated with the features indicated as the reflected (driver) expansion and the piston stopping shock in Fig. 5a are well simulated for the nitrogen test gas condition. For the carbon dioxide simulation, the magnitude of these pressure changes is somewhat different from the measured values (Fig. 6a) and, in the case of the piston stopping shock, its arrival is late (relative to the measurements) by approximately 1.5ms. Because the carbon dioxide condition required a substantially higher air driver pressure than the nitrogen test gas condition, it is possible that the actual initial driver temperature was higher than 321K (the value used in the simulations) - see Section 2.3.

4.2 Temperature

The simulated pressure levels behind the incident shock for both the nitrogen and carbon dioxide conditions is within 2% of the measured values. However, the simulated and experimental reflected shock pressure levels differ by up to 7% (the worst case being the carbon dioxide condition immediately following shock reflection). This difference leads to an underestimation of the flow stagnation temperature (see Fig. 6b) during the initial portion of the gun tunnel flow (up to about 0.04s). During the test time indicated in Fig. 5 and 6, the average difference between the simulated and measured temperatures is 2.5% for the nitrogen condition and 0.8% for the carbon dioxide condition. The exceptional agreement of temperatures in the carbon dioxide case arises because of cancellation of errors. The simulation underestimates both the shock-induced temperature rise and the barrel heat losses.

For many years it has been known that barrel heat transfer can influence the stagnation temperatures achieved in gun tunnels, [Edney (1967)]. Convective cooling of the test gas during the compression stroke is the mechanism primarily responsible for the observed decay in test gas temperature leading up to, and during the test time. Given the approximate nature of the heat transfer model used in the simulation (a fully developed pipe flow model), some discrepancy between the simulated and experimental measurements is expected. In an attempt to improve the simulated temperatures, a turbulent flat plate boundary layer model was implemented in the Lagrangian formulation to calculate the viscous losses and heat transfer from the test gas during the compression process. However, the turbulent flat plate boundary layer model did not significantly improve the accuracy of the simulation. Both the pipe flow and the flat plate models underestimated the heat loss from the test gas during gun tunnel operation.

5 Conclusion

The quasi-one-dimensional calculation requires gradual area variations along the length of the simulated facility for accurate prediction of flow discharge. However, actual facility area variations are often rapid and need to be modelled as such if wave reflection processes are to be simulated accurately.

Contraction profiles based on the control-mass cells experiencing either (1) a rate of length increase at a constant fraction of the local flow velocity or (2) a constant fractional area change, both produce similar profiles. These profiles produce a very rapid initial contraction which is useful for simulating shock reflection at the end of the barrel, but the contraction becomes gradual as the throat is approached. For simulating the flow discharge through the Mach 7 gun tunnel nozzle with an accuracy of better than 1%, it was necessary to ensure that the rate of cell-length increase was less than about 13% of the local flow velocity, or the area change across each cell was less than about 9% throughout the contraction.

The current work demonstrates that an accurate simulation of the gun tunnel barrel pressures (with an average deviation from the measurements of around 3%) can be achieved by tuning the simulated pressure losses in the driver-barrel transition region. Having tuned the pressure simulation in this manner, it is also demonstrated that the simulated flow stagnation temperatures are on average within about 3% of experimental measurements. Furthermore, the pressures and temperatures at a different operating condition are also simulated with a similar level of accuracy.

Although the simulation currently underestimates the barrel heat losses, the comparisons suggest that the Lagrangian formulation could be used to predict the thermodynamic state of the test gas throughout the duration of the gun tunnel flow with an uncertainty of around 5%. The current results provide additional evidence that the Lagrangian model can be used as a predictive tool for impulse facility design and flow condition identification.

Acknowledgement DRB wishes to acknowledge the financial support of an EPSRC Visiting Fellowship which enabled the acquisition of the carbon dioxide data reported in this article.

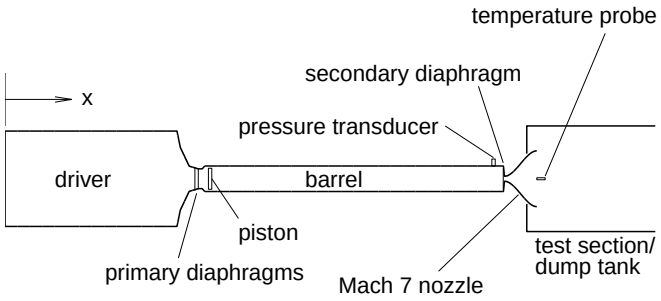

Figure 1: Schematic illustration of the Oxford University Gun Tunnel.

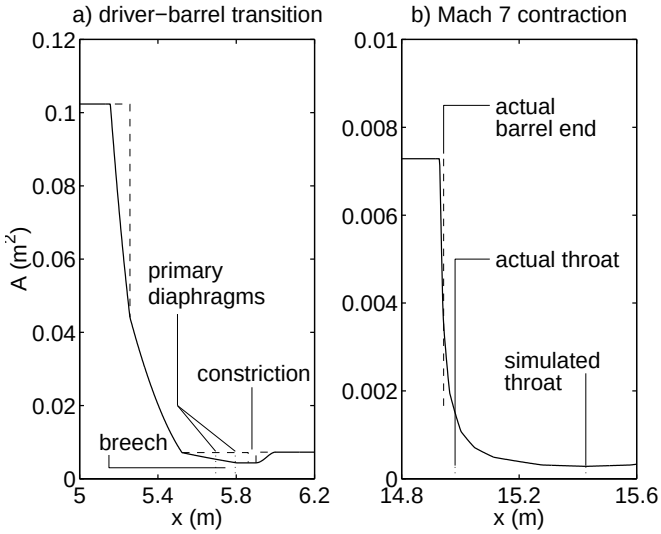

Figure 2: Facility area variation in the driver-barrel transition region and the Mach 7 nozzle contraction. Solid line: distribution used in simulation; broken line: closer approximation to actual distribution.

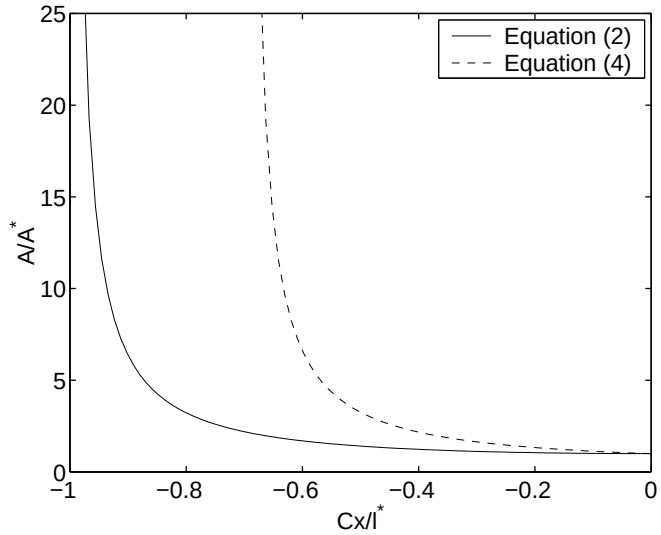

Figure 3: Area distribution for contractions designed using (2) and (4), with $\gamma = 1.4$.

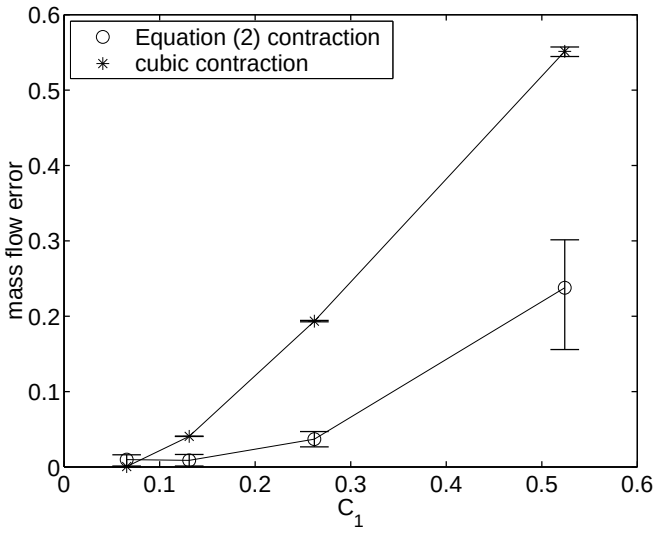

Figure 4: Mach 7 nozzle mass flow error as a function of C_1.

Table 1: Principal dimensions of the Oxford University Gun Tunnel

Region	Length (m)	Diameter (mm)
Driver	5.257	361
Transition	0.644	237 (inlet)
		74.5 (constriction)
Barrel	9.042	96.3
Mach 7 Nozzle	1.003	19.05 (throat)
		211 (exit)

Table 2: Initial filling pressures for the two conditions

Test gas	Air Driver (MPa)	Barrel (kPa)
Nitrogen	4.90±0.15	162±2
Carbon Dioxide	7.70±0.15	194±3

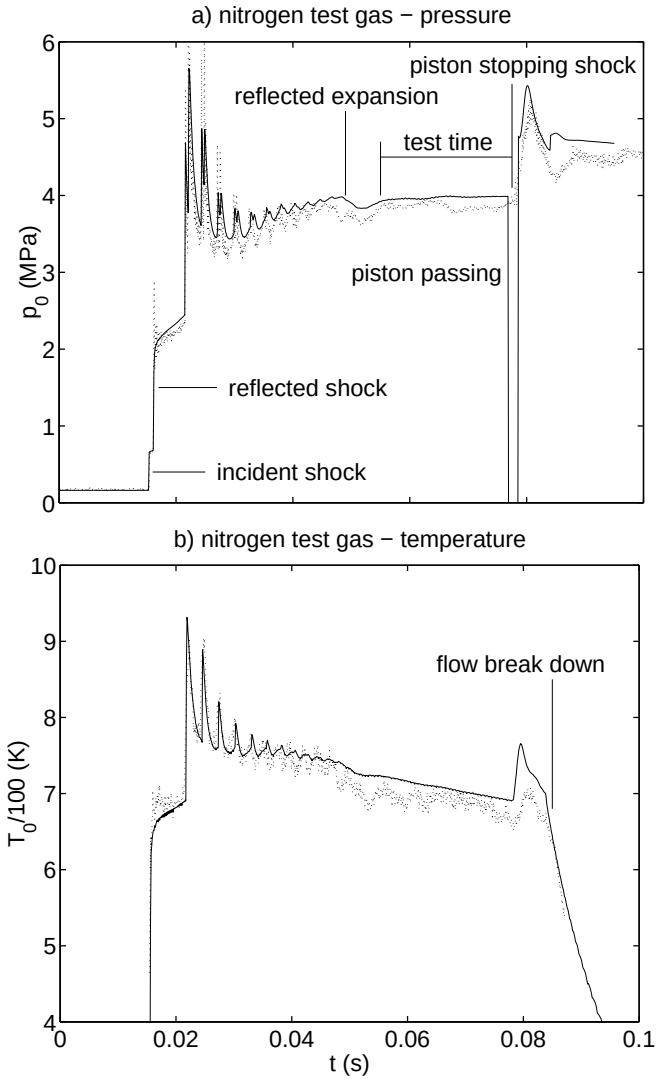

Figure 5: Comparison of measurements (dots) and simulations (solid line) for the nitrogen test gas condition.

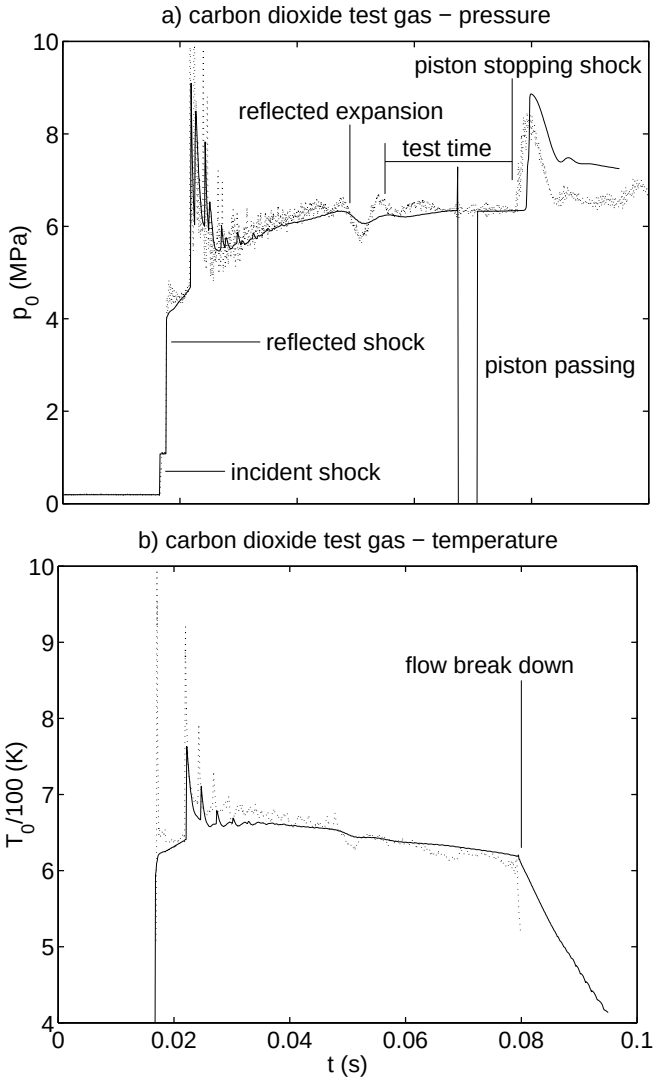

Figure 6: Comparison of measurements (dots) and simulations (solid line) for the carbon dioxide test gas condition.

References

[Buttsworth and Jones (1998)] Buttsworth DR, Jones TV (1998) A Fast-Response Total Temperature Probe for Unsteady Compressible Flows. J. Eng. for Gas Turbines and Power 120:694–702

[Chang and Kim (1995)] Chang K-S, Kim J-K (1995) Numerical investigation of inviscid shock wave dynamics in an expansion tube. Shock Waves 5:33–45

[Doolan and Jacobs (1996)] Doolan CJ, Jacobs PA (1996) Modeling mass entrainment in a quasi-one-dimensional shock tube code. AIAA Journal 34:1291–1293

[Edney (1967)] Edney, BE (1967) Temperature measurements in a hypersonic gun tunnel using heat transfer methods. J Fluid Mech 27:503–512

[Groth et al. (1991)] Groth CPT, Gottlieb JJ, Sullivan PA (1991) Numerical investigation of high-temperature effects in the UTIAS-RPI hypersonic impulse tunnel. Canadian Journal of Physics 69:897–918

[Jacobs (1992)] Jacobs PA (1992) An approximate Riemann solver for hypervelocity flows. AIAA Journal 30:2558–2561

[Jacobs (1994)] Jacobs PA (1994) Quasi-one-dimensional modeling of a free-piston shock tunnel. AIAA Journal 32:137–145

[Petrie-Repar and Jacobs (1998)] Petrie-Repar PJ, Jacobs PA (1998) A computational study of shock speeds in high-performance shock tubes. Shock Waves 8:79–91

[Roache (1994)] Roache, PJ (1994) A method for uniform reporting of grid refinement studies. J Fluids Engineering 116:405–413

[Tani et al. (1994)] Tani K, Itho M, Takahashi M, Tanno T, Komuro T, Miyajima H (1994) Numerical study of free-piston shock tunnel performance. Shock Waves 3:313–319